J. Fluid Mech. (1997), *vol.* 335, *pp.* 165–188

On the theory of electrohydrodynamically driven capillary jets

By ALFONSO M. GAÑÁN-CALVO

Grupo de Mecánica de Fluidos, Escuela Técnica Superior de Ingenieros Industriales, Universidad de Sevilla, 41012 Sevilla, Spain

(Received 8 December 1995 and in revised form 2 October 1996)

Electrohydrodynamically (EHD) driven capillary jets are analysed in this work in the parametrical limit of negligible charge relaxation effects, i.e. when the electric relaxation time of the liquid is small compared to the hydrodynamic times. This regime can be found in the electrospraying of liquids when Taylor's charged capillary jets are formed in a steady regime. A quasi-one-dimensional EHD model comprising temporal balance equations of mass, momentum, charge, the capillary balance across the surface, and the inner and outer electric fields equations is presented. The steady forms of the temporal equations take into account surface charge convection as well as Ohmic bulk conduction, inner and outer electric field equations, momentum and pressure balances. Other existing models are also compared. The propagation speed of surface disturbances is obtained using classical techniques. It is shown here that, in contrast with previous models, surface charge convection provokes a difference between the upstream and the downstream wave speed values, the upstream wave speed, to some extent, being delayed. Subcritical, supercritical and convectively unstable regions are then identified. The supercritical nature of the microjets emitted from Taylor's cones is highlighted, and the point where the jet switches from a stable to a convectively unstable regime (i.e. where the propagation speed of perturbations become zero) is identified. The electric current carried by those jets is an eigenvalue of the problem, almost independent of the boundary conditions downstream, in an analogous way to the gas flow in convergent–divergent nozzles exiting into very low pressure. The EHD model is applied to an experiment and the relevant physical quantities of the phenomenon are obtained. The EHD hypotheses of the model are then checked and confirmed within the limits of the one-dimensional assumptions.

1. Introduction

Electrohydrodynamically (EHD) driven capillary jets and their stability has attracted the attention of many investigators since the first works on the stability of capillary jets (Rayleigh 1878; Weber 1931). This kind of liquid flow appears when strong electric fields are applied to liquid masses, or when a liquid is injected under the effect of an external electric field. The eventual breakup of these liquid jets into droplets, which usually have diameters several orders of magnitude smaller than the droplets from uncharged jet breakup, was essentially the objective of their analysis.

The electrohydrodynamic atomization of liquids (or electrospray) actually comprises multidisciplinary aspects from electrostatics, electrokinetics, fluid dynamics, particle dynamics, etc. From the pioneering presentations of Zeleny (1914, 1915, 1917), and

Vonnegut & Neubauer (1952), many experimental works have been devoted to the determination of the physical laws relating the liquid properties and flow rate to the size and charge of the emitted droplets (Hendricks 1962, 1964; Pfeifer & Hendricks 1967, 1968; Jones & Thong 1971; Hayati, Bailey & Tadros 1986*a*, *b*; Cloupeau & Prunet-Foch 1989, 1990; Tang & Kebarle 1991; Fernández de la Mora & Loscertales 1994; Gañán-Calvo, Dávila & Barrero 1997, among many others) as well as to describing the nature and structure of the resulting spray (Dunn & Snarski 1992; Gomez & Tang 1994; Tang & Gomez 1994; Gañán-Calvo *et al.* 1994, among others).

Melcher & Warren (1971) analysed the electrohydrodynamics of a steady, semi-insulating liquid jet pulled down under the action of a tangential electric field and gravity, in order to supply an analytical model to understand the experiments performed by Taylor (1969). In that work, they introduced realistic assumptions related to the electrohydrodynamics of the microjet in electrosprays (e.g. the relaxation time of liquid charges is small compared to hydrodynamic residence times), wrote down the appropriate axial momentum and normal force balance, etc. However, they did not arrive at significant scaling laws for the emitted current or droplet size since, to close their model, Melcher & Warren artificially imposed an external linear electric field instead of scaling the axial electric field as that due to the accelerating jet itself (self-induction). Furthermore, they did not retain the convective terms in the total electric current carried by the jet. Actually, in electrohydrodynamically driven jets which eventually break up into droplets and form a charged spray this current is not a parameter, but on the contrary, it is a *result* for the given control parameters (potential difference and liquid flow rate). However, leaving aside its application to the electrospray phenomenon, their EHD model was physically very rich since they discovered the existence of EHD subcritical and supercritical flow regimes. In fact, the breakup point of the jet has no influence upstream if the jet flow is supercritical, and the system may exhibit a steady-state regime if the boundary conditions upstream of the jet are steady. They also obtained a fundamental surface charge conservation equation in electrohydrodynamic spraying (equation (9), in their work). Although the work by Melcher & Warren may be considered a major cornerstone of electrospray science, it seems that not enough attention has been devoted to their analysis in this field.

More recently, Turnbull (1989) presented an electrohydrodynamic model for the emitted jet in the limits of both perfectly insulating and perfectly conducting liquids. He obtained the scaling of the jet radius, leaving the emitted current as an input. In an approximate solution of his equations, he assumed (p. 703, 2nd paragraph) a negligible surface tension since it would have "not reached its equilibrium value" along the jet. This assumption, although not entirely justified for the experimental conditions in most electrospray measurements reported in the literature, has also been considered very recently by Mestel (1994) among other theoretical hypotheses. Mestel performed a stability analysis of a charged jet subjected to a given axial electric field, undergoing small perturbations, assuming a finite electrical relaxation time and a high-Reynolds-number model for the resulting perturbation motions. His analysis covers a wide range of parametrical situations, among which his limit of a low tangential field is suggested as the most plausible one from the point of view of its application to the cone–jet mode. In fact, this is essentially correct as the experiments show. In these conditions, he shows that the jet is stabilized by the low shear stress electrically exerted on its surface, which is compatible with most experimental observations.

This work is devoted to the analysis of electrohydrodynamically driven jets in the parametrical limits of negligible charge relaxation effects, i.e. when charge relaxation time ε_i/K is small compared to other times of interest in the problem, ε_i and K being the electrical permittivity and conductivity of the liquid, respectively. This limit holds for electrospraying in the steady jet regime for liquid flow rates large compared to the minimum one for which the jet is steady. If the liquid is issuing from a needle of a small enough diameter, and the flow rate is large, the microjet is almost quasi-unidirectional from the beginning. If, on the contrary, the liquid flow rate is small and the needle's diameter is moderate, the liquid is usually emitted in cone–jet mode (Cloupeau & Prunet-Foch 1989); in this regime, there is a region (the cone) which is essentially electrostatic, which breaks down abruptly at its apex, forming a microjet with markedly different characteristics (not negligible tangential electric field on the surface, large liquid velocities, etc.) from those of the cone. To analyse such a flow, the capillary forces, hydrodynamic pressure, electric forces, viscous forces, and momentum of the liquid are retained in the normal and tangential EHD balance equations. In addition, both the surface convection and the bulk conduction currents are taken into account in the total emitted current. Following Melcher & Warren's work, the flow is analysed here in terms of the propagation speed of surface disturbances. In §2, two different kinds of external boundary conditions, leading to different solutions of the external electric field and resulting flow characteristics, are also analysed. Retaining the self–induction effects, it is shown that the microjet may undergo a transition from a subcritical regime (upstream) to a supercritical one (downstream), which is forbidden for jets with no self-induction (Melcher & Warren's ones).

The quasi-unidirectional EHD model presented here is applied to an experiment in §3, and the hypotheses made are checked. Based on the facts revealed by this experiment, it is suggested that the conspicuous stability and steadiness of the conical meniscus and emitted microjet in the parametrical limits of stability for the steady cone–jet mode is related to the effect of a *supercritical shield* supplied by the microjet behind the point where the propagation speed of perturbations becomes imaginary (i.e. where the jet becomes convectively unstable). From this point, the small perturbations grow exponentially, leading eventually to the jet breakup. In addition, all other relevant physical quantities such as the normal and tangential electric fields, electrostatic forces, polarization forces, pressure, liquid inertia, Ohmic bulk conduction current, surface charge advection current, etc., are experimentally quantified within the errors of the quasi-one-dimensional model, allowing for a direct verification of the electrohydrodynamical hypotheses.

1.1. *Preliminary notes and limits of validity of the theory*

If the liquid has a sufficiently high electrical conductivity or, in other words, a sufficient concentration of charge carriers with large enough electrical mobility compared to other velocities of the problem, there is a layer in the liquid at the liquid–gas interface whose charge distribution in the direction normal to the interface is given by the electrochemical equilibrium of the charge carriers present in the liquid, under the effect of the electric fields. When the charge carriers are ions, this charge distribution is given by the well-known Poisson–Boltzmann equation (see, for example, Probstein 1989, p. 100), and its thickness is of the order of a Debye length in a perfect equilibrium state. If the liquid is slowly flowing, in a Lagrangian framework (following the liquid particles) the surface charge layer is always in a quasi-equilibrium state whenever mechanical and geometrical variations take place slowly enough to allow for the surface charge layer to 'accommodate' almost instantaneously to the slow changes

occurring in the flow (like in the local thermodynamic equilibrium hypothesis). This is the limit scenario considered in the present work, which can be referred to as the limit of negligible charge relaxation effects. In this case, in terms of characteristic times, the electric relaxation time $\beta\varepsilon_o/K$ is small compared to other times of interest, say the hydrodynamic residence time of a liquid particle in the jet $t_o \sim L/U \sim LR_j^2/Q$, where β, K, L, R_j, U and Q are the liquid to the vacuum electrical permittivities ratio, the liquid electrical conductivity, a characteristic jet length (say, from the cone's apex down to the breakup point), a jet diameter (say, close to the breakup point, where it is minimum), the typical liquid axial velocity, and the liquid flow rate, respectively. That is,

$$\frac{\beta\varepsilon_o Q}{KR_j^2 L} \ll 1. \tag{1.1}$$

The most important fact related to the requirement of negligible charge relaxation effects is that the inner, normal electric field multiplied by β should be very small compared to the outer, normal electric field ($E_n^o \gg \beta E_n^i$) (see Probstein 1989). In fact, for a perfect equilibrium state, the inner electric field becomes exactly zero. This is the case of a perfectly quiescent liquid (no flow) with a liquid–gas interface under the influence of an external, constant electric field, or the case of a perfectly conducting liquid. It is precisely the existence of a tangential electric field on the jet's surface that stops it being in a 'perfect' equilibrium: it provokes a progressive acceleration of the liquid and the consequent decreasing of the jet radius. Thus, there is a slow motion of the liquid, moving with the average axial velocity (albeit the tangential electric field should be small enough to keep conditions quasi-static when moving with the liquid). Another implication of the assumption of an EHD surface quasi-equilibrium condition is the use of the classical, static form of the capillary equilibrium condition with the static value of the surface tension γ (Landau & Lifshitz 1960, §15).

Furthermore, the surface tangential electric stress $\tau_e \sim \mu\Delta U/R_j$ (where ΔU is the typical transversal variation of the liquid velocity $U \sim Q/R_j^2$) is of the order of $\rho U^2 R_j/L \sim \rho Q^2/(R_j^3 L)$. If this surface stress is small as compared to $\mu U/R_j \sim \mu Q/R_j^3$, the axial velocity profile of the liquid is almost flat (see Melcher & Warren 1971, pp. 130–131, and 142; Fernández de la Mora & Loscertales 1994, p. 183; Mestel 1994, pp. 95–96; Gañán-Calvo *et al.* 1994) since the transversal velocity variation ΔU is small compared to U. This is accomplished if the viscous diffusion of momentum from the surface is efficient, since the larger the viscosity, the flatter the velocity profile for a given flow rate and surface stress, or alternatively: if the viscous diffusion time across the jet $t_v \sim R_j^2/\nu$ is of the order of, or smaller than, the hydrodynamic residence time t_o:

$$t_o \gtrsim t_v \Longrightarrow \frac{Q}{\nu L} \lesssim 1 \tag{1.2}$$

(where ν is the liquid kinematic viscosity), the vorticity is sufficiently diffused across the jet's section, and its value is small compared to $U/R_j \sim Q/R_j^3$. Within this limit, a liquid portion of the jet can be followed in a Lagrangian framework moving with the local, axial velocity of the liquid, with respect to which the liquid may be considered almost quiescent. It is noteworthy that in this limit the liquid viscosity disappears from the equations if the axial component of the viscous diffusion $\mu\partial^2 v_z/\partial z^2 \sim \mu U/L^2$ (where z stands for the axial coordinate, and v_z is the liquid velocity in the z-direction, see Melcher & Warren 1971, pp. 133 and 142) is small compared to the variations of

the liquid inertia along the jet:

$$\rho\frac{U^2}{L} \gg \mu\frac{U}{L^2} \Longrightarrow \frac{Q}{\nu L} \gg \left(\frac{R_j}{L}\right)^2 \tag{1.3}$$

where ρ is the liquid density, $\mu = \rho\nu$, and L is a characteristic axial length. In conclusion, we have that

(i) charge relaxation effects are negligible if $\dfrac{\beta\varepsilon_o Q}{K R_j^2 L} \ll 1$;

(ii) viscous effects are negligible if

$$\left(\frac{R_o}{L}\right)^2 \ll \frac{Q}{\nu L} \lesssim 1. \tag{1.4}$$

In §3, both conditions are checked for a real electrohydrodynamically driven jet.

The problem will be solved in the absence of ion emission or corona discharge phenomena. A thorough discussion on this particular subject can be found in Cloupeau (1994, pp. 1150–1152).

2. Formulation of the problem

A semi-insulating liquid with electrical conductivity and permittivity K and ε_i, respectively, is issuing in the form of a steady, slender capillary jet from an injecting needle or a circular orifice of radius R_a. There is an electric potential difference $\Delta\phi_o$ (a control parameter of the problem) between the needle and the surroundings, generally a grounded electrode located in front of the needle, so that there is an 'external' electric field applied along the jet direction, and the jet is bearing an electric charge. Some configurations of the electrohydrodynamically driven jets considered in this work are given in figure 1. The liquid flow rate Q is kept constant as a given parameter (another control parameter) of the problem. Other physical relevant parameters of the problem are the liquid-gas surface tension γ, and the liquid density and viscosity, ρ and μ, respectively. As a result of the electric charge carried by the jet, there will be a net electric current I circulating from the injecting needle (or orifice) towards the external electrode. There are two possibilities:

(i) The jet is continuous and strikes the electrode before breaking up into droplets. This problem was considered by Melcher & Warren (1971). The charge is then circulated to the electrode by both bulk Ohmic conduction along the jet and surface charge convection, although the latter was neglected by Melcher & Warren in their model.

(ii) The jet breaks up into charged droplets which travel towards the electrode under the external electrostatic field's force. The electric current is then entirely convected by the droplets.

In either case, the electric current I is a result of the potential difference $\Delta\phi_o$ between the jet's base and the electrode. In the case of Melcher & Warren, the values of $\Delta\phi_o$ for which their jets are steady range from 0 to several kilovolts, being the upper limit determined by asymmetric instabilities or gas discharges. The jet acts almost as an electric resistance between the charged needle and the electrode: there is an almost linear relation between the voltage drop and the electric current. Thus, either $\Delta\phi_o$ or I may be taken as the control parameter: given one of them, the other is determined. In the second scenario, the necessary potential differences are of the order of kilovolts, but the *range* of these potential differences for which the jet is

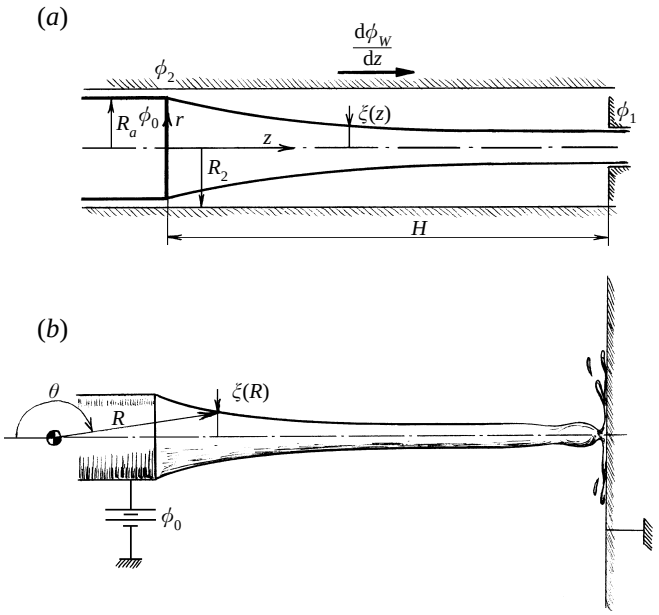

FIGURE 1. (*a*) Configuration, coordinates, and dimensions for the extension of Melcher & Warren's model, where $\Delta\phi_o = \phi_o - \phi_1$, and $\Delta\phi_1 = \phi_o - \phi_2$. (*b*) Configuration, coordinates, and dimensions in the analysis of Taylor's jet.

steady is greatly reduced to a few hundreds of volts (Zeleny 1915, 1917; Jones & Thong 1971; Mutoh, Kaieda & Kamimura 1979; Smith 1986; Cloupeau & Prunet-Foch 1989, 1990; among many others). In this case, the electric current I is no longer a control parameter since the potential difference is almost fixed, and I becomes an eigenvalue of the problem, depending almost entirely on the liquid physical properties and the liquid flow rate Q (Cloupeau and Prunet-Foch 1989; Fernández de la Mora & Loscertales 1994).

The slender geometry of the jet will allow a dramatic simplification of the equations. We will first derive the equations retaining the non-steady terms in order to understand the basic phenomena involved in the propagation of disturbances along the jet, similarly to the model presented by Melcher & Warren (1971). This will be essential for the discussion of the global stability of the jet and the existence of a cut-off flow rate: while the flow remains supercritical (liquid velocity larger than the propagation speed of perturbations), the strong perturbations due to the jet breakup cannot proceed upstream and the jet stays almost unperturbed up to the breakup region. For the existence of such a supercritical flow, the existence of a critical point is necessary at the exit of the feeding needle at which the flow accelerates from a subcritical to a supercritical regime. This supercritical flow is almost insensitive to downstream perturbations or boundary conditions. However, when the parametrical limit for the existence of such a critical point is reached, the supercritical shield disappears and the whole flow becomes affected by the jet breakup. In this situation, the whole jet is no longer stable (global instability). An analogous phenomenon, rather common and observed by anyone, is the minimum flow rate for which a laminar, capillary, steady jet issuing from a tap suddenly bifurcates to a dripping mode, which was described theoretically by Bogy (1981).

2.1. *One-dimensional model equations*

The jet is assumed to have axial symmetry along its direction of propagation. Thus, except when otherwise stated, we will use cylindrical coordinates (r, z) to describe the jet's motion and geometry, and all dependent variables are in general functions of the axial position z and time t.

The jet's shape is described by a function ξ satisfying

$$\xi - r = 0 \tag{2.1}$$

where, owing to the slenderness of the jet, its characteristic axial length L is large compared to its typical radius $R_o \sim O(\xi)$.

Owing to the electric potential difference between the jet and the surroundings, the jet is bearing a charge σ_e per unit length equal to

$$\sigma_e = 2\pi\xi\varepsilon_o \left[E_n^o - \beta E_n^i\right] \tag{2.2}$$

where $\beta = \varepsilon_i/\varepsilon_o$ is the permittivies ratio between the liquid and the vacuum. E_n^o and E_n^i are the outer and inner normal electric fields on the jet's surface.

In addition, the jet is subject to an axial electric field E_z and, therefore, the liquid–gas interface undergoes an electric tangential stress given by

$$\tau_e = E_z\varepsilon_o(E_n^o - \beta E_n^i) \approx \varepsilon_o E_n^o E_z \tag{2.3}$$

under the assumption $\beta E_n^i \ll E_n^o$. Thus, following Melcher & Warren in assuming an almost flat velocity profile $v \approx Q/(\pi\xi^2)$ (under conditions given in §1.1) the mass, momentum and charge conservation equations read

$$\frac{\partial \xi^2}{\partial t} + \frac{\partial}{\partial z}(\xi^2 v) = 0, \tag{2.4}$$

$$\left(\frac{\partial}{\partial t} + v\frac{\partial}{\partial z}\right) v + \frac{1}{\rho}\frac{\partial p}{\partial z} = \frac{2\varepsilon_o E_z E_n^o}{\rho\xi}, \tag{2.5}$$

$$\xi\left(\frac{\partial}{\partial t} + v\frac{\partial}{\partial z}\right) E_n^o + \frac{K}{2\varepsilon_o}\frac{\partial}{\partial z}(\xi^2 E_z) = E_n^o\left(\frac{\partial}{\partial t} + v\frac{\partial}{\partial z}\right)\xi, \tag{2.6}$$

respectively. p and v are the local thermodynamic pressure and axial velocity of the liquid, respectively, and the pressure jump across the jet's surface must obey the capillary equation:

$$p - p_a = \frac{\gamma}{\xi} - \frac{\varepsilon_o}{2}\left[(E_n^o)^2 + (\beta - 1)E_z^2\right] \tag{2.7}$$

where $p_a = const.$ is the outside gas pressure. From now on, and without lost of generality, we will write $p - p_a$ simply as p.

The outer electric field is given by the equation

$$\nabla \cdot \boldsymbol{E}^o = 0 \tag{2.8}$$

with boundary conditions. This equation and boundary conditions close the problem since they formally supply a relationship between the outside, normal component E_n^o and the tangential component E_z of the electric field at the jet's surface. However, is not always possible to write a closed expression for the relationship between E_z and E_n^o owing to the complexity of the external boundary conditions (needle, collector, and surrounding geometries and potentials). It is at this point where an important feature of the problem arises: whether or not the electric self-induction on the jet is

allowed for. It will be shown that Taylor's jets (the ones issuing from the so-called Taylor's cones) are genuinely self-inductive.

Finally, once the tangential component E_z is known, the inner electric field can be calculated under the assumption that free charges are absent from the liquid bulk, and stay in a quasi-equilibrium surface charge layer. The solution of the inner electric field, satisfying the Laplacian, gives

$$E_n^i + \frac{1}{2\xi}\frac{\partial}{\partial z}(\xi^2 E_z) = 0 \tag{2.9}$$

owing to the slenderness of the jet's geometry ($L \gg R_o$).

2.2. *No self-induction external electric field on the jet: an extension of Melcher & Warren's model*

In order to overcome the problem of finding a closed expression for the tangential electric field on the jet's surface, Melcher & Warren (1971) studied a particular configuration for which the tangential electric field was imposed by a cylindrical electrode concentrically surrounding the jet (figure 1*a*). This electrode, subject to a potential difference, presented a linear potential decay along its axis, such that

$$E_{zW} = -\frac{\mathrm{d}\phi_W}{\mathrm{d}z} = \text{const.} \tag{2.10}$$

where ϕ_W is the cylindrical electrode's potential. If its position is given by $r = R_2$, the tangential electric field E_z on the jet's surface can be expressed in closed form as

$$E_z = \xi \log\left(\frac{\xi}{R_2}\right)\frac{\partial E_n^o}{\partial z} + E_n^o\left[1 + \log\left(\frac{\xi}{R_2}\right)\right]\frac{\partial \xi}{\partial z} + E_{zW}. \tag{2.11}$$

Melcher & Warren's rather pioneering model differs from the present one in that the convective charge variations in equation (2.6) are now retained. In order to clarify the statement made by these authors that an electric relaxation time ε_o/K 'short compared to times of interest,' (say t_o) reduces equation (2.6) 'to its last term, which is then integrated to obtain:' $E_z = I/(K\pi\xi^2)$, where I is the total electric current carried by the jet (Melcher & Warren 1971, p. 133) it should be pointed out that their simplification is valid as long as the characteristic axial and transversal lengths of the problem are comparable. However, for slender jets, an estimation of the orders of magnitude of the two terms in equation (2.6) does not allow the neglect of the first term when $K/\varepsilon_o \gg t_o^{-1}$, since $L \gg R_o$. In fact, the first term in (2.6) is of $O((\phi_s - \phi_W)/t_o) \sim O(\phi_W/t_o)$, while the second one is $O((K/\varepsilon_o)(R_o^2/L^2)\phi_W)$. Therefore the ratio between the two terms is of the order of

$$\frac{\varepsilon_o}{K t_o}\frac{L^2}{R_o^2} \tag{2.12}$$

which is not necessarily small, even though $\varepsilon_o/K \ll t_o$.

The condition of negligible charge relaxation effects ($\beta E_n^i \ll E_n^o$) allows a drastic simplification of capillary equation (2.7) since the effect of the inner electric field can be neglected in this limit, and the coupling between equations (2.7) and (2.9) disappears. Therefore, equations (2.4), (2.5), (2.6) and (2.11) define a system of four first-order partial differential equations with characteristic equations like the one found by Melcher & Warren (see also Shapiro 1953, p. 73). Focusing our attention on the axisymmetric perturbations within the limit (1.1), i.e. perturbations with a

wavelength λ such that $R_o \ll \lambda \ll L$, but still

$$\frac{\beta Q \varepsilon_o}{K R_o^2 \lambda} \ll 1, \tag{2.13}$$

we deal with non-dispersive, quasi-one directional waves only. Their propagation speed a (as usual, with respect to the moving liquid), interestingly enough, is *slower* in the upstream direction (say a^-) than in the downstream direction (say a^+). The result is the same as that found by Melcher & Warren, given by

$$a_{MW} = \left\{ \frac{\varepsilon_o}{2\rho} \left[1 + \frac{1}{\log(\xi/R_2)} \right] (E_n^o)^2 + \frac{\varepsilon_o(\beta - 1)}{\rho} E_z^2 - \frac{\gamma}{2\rho\xi} \right\}^{1/2} \tag{2.14}$$

except for the appearance of a new term, a_{CC}, due to the non-zero surface charge convection. The resulting wave speed can be written in the form

$$a^{\pm} = \pm a_{CC} + (a_{MW}^2 + a_{CC}^2)^{1/2} \tag{2.15}$$

where

$$a_{CC} = \frac{\varepsilon_o^2(\beta - 1) E_n^o E_z}{2\rho K \xi} \left[2 + \frac{1}{\log(\xi/R_2)} \right]. \tag{2.16}$$

The additional term is, however, small compared to a_{MW} except for high-polarity liquids ($\beta \gg 1$). A detailed derivation of the propagation speed a and its limits of applicability is given in Appendix A.

As long as this wave speed is real, the jet is locally and convectively stable, but should a^- become complex (i.e. when $a_{MW}^2 \leqslant a_{CC}^2$), with a non–zero imaginary part equal to $(a_{CC}^2 - a_{MW}^2)^{1/2}$, the jet become convectively unstable, in the sense that small perturbations grow exponentially in time when moving at the average jet velocity (*convective* instability). It should be repeated that $|a_{CC}|$ is small compared to the wave speed $|a_{MW}|$ or the liquid velocity $v = Q/(\pi\xi^2)$ in the supercritical region for moderate-permittivity liquids, as will be shown in §3. In these cases, $a^2 \approx a_{MW}^2$, and the jet becomes unstable, within a good approximation, at the point where a_{MW}^2 becomes negative.

The steady form of system (2.4), (2.5), (2.6), (2.7) and (2.11) within the limit (1.1) can be reduced to a system of two first-order ordinary differential equations given by

$$\left[\frac{2\varepsilon_o(\beta - 1)}{\rho} E_z^2 - \left(\frac{Q}{\pi} \right)^2 \frac{2}{\xi^4} - \frac{\gamma}{\rho\xi} \right] \frac{1}{\xi} \frac{\mathrm{d}\xi}{\mathrm{d}z} - \frac{\varepsilon_o E_n}{\rho} \frac{\mathrm{d}E_n^o}{\mathrm{d}z} = \frac{2\varepsilon_o E_z E_n^o}{\rho\xi} \tag{2.17}$$

together with equation (2.11). E_z is obtained from the steady, integral form of equation (2.6):

$$I = K\pi\xi^2 E_z + \frac{2Q\varepsilon_o E_n^o}{\xi} \tag{2.18}$$

where I is the total electric current. In explicit form, one has

$$\frac{\mathrm{d}\xi}{\mathrm{d}z} = \frac{-\varepsilon_o E_n^o \left[E_z \left(1 + 2\log\left(\frac{\xi}{R_2} \right) \right) - E_{zW} \right]}{2\rho \log\left(\frac{\xi}{R_2} \right) (v + a^+)(v - a^-)}, \tag{2.19}$$

$$\frac{\mathrm{d}E_n^o}{\mathrm{d}z} = \frac{\varepsilon_o E_z (E_n^o)^2 \left[1 + \log\left(\frac{\xi}{R_2}\right)\right] - \left[\varepsilon_o(\beta - 1)E_z^2 - \rho\left(\frac{Q}{\pi}\right)^2 \frac{1}{\xi^4} - \frac{\gamma}{2\xi}\right](E_z - E_{zW})}{\rho\xi \log\left(\frac{\xi}{R_2}\right)(v + a^+)(v - a^-)}. \tag{2.20}$$

In these expressions, $v = Q/(\pi\xi^2)$ is the liquid velocity, E_z is obtained from (2.18), and $a^{\pm}$ is given by expression (2.15). The total electric current I is an eigenvalue of the problem, which is solved using the integral condition:

$$\int_0^L E_z(z)\mathrm{d}z = \Delta\phi_o \tag{2.21}$$

where $\Delta\phi_o$ is the potential difference between the needle and the plate the jet finally meets. The boundary conditions

$$\xi(0) = R_a \quad \text{and} \quad E_n^o(0) = \frac{\Delta\phi_1}{R_a \log(R_a/R_2)} \tag{2.22}$$

finally determine the solution of the problem, where R_a is the feeding needle's radius, and $\Delta\phi_1$ is the value of the potential difference between the needle and the cylindrical electrode at the origin (see figure 1*a*).

As Melcher & Warren pointed out, the flow can be either subcritical or supercritical depending on whether a^- is larger or smaller than v, respectively (a^- and v being considered real and positive). Although this problem was analysed by Melcher & Warren in the limit of a negligible surface charge convection ($a_{CC} \equiv 0$), the importance of the identification of such regimes becomes apparent on analysing experimentally the global stability of the flow (there is an interesting educational film on this subject made by these authors).

While v is smaller than a^-, the flow is locally subcritical, and switches to a supercritical regime for v larger than a^-. This simple picture, however, is not so straightforward if one analyses expressions (2.19) and (2.20): the flow must cross a point where $a^- = v$, and equations (2.19) and (2.20) become singular. The condition that $\mathrm{d}\xi/\mathrm{d}z$ and $\mathrm{d}E_n^o/\mathrm{d}z$ must be finite (both nominator and denominator in the right-hand-side terms be zero at the singular point) leads to the characterization of the critical or *transonic* point. Why Melcher & Warren could not find a critical point (*transonic* flow) with their model can be seen from equation (2.19): both numerator and denominator of the right-hand-side term should be simultaneously zero at the critical point; however, it is impossible since $E_z[1 + 2\log(\xi/R_2)]$ is always *smaller* than E_{zW}. E_z must be positive in order to have a decreasing potential along the jet (the contrary is an absurdity), and the driving external axial electric field E_{zW} is also positive; there is no point in the (positive) phase space (ξ, E_n^o) for which both numerators in equations (2.19) and (2.20) become simultaneously zero in these conditions. Thus, the numerator in equation (2.19) is *always negative*, while the denominator can vanish at a certain point, but since it would lead to a local infinite slope, such a point cannot exist in the range $0 < z < L$.

In conclusion, Melcher & Warren's jets are either subcritical or supercritical from the very beginning ($z = 0$) up to the point where they impinge on the final electrode ($z = L$), or up to the point z^* where they become unstable ($a_{MW}^2(z^*) = 0$). The most important result from Melcher & Warren's model in connection with the EHD spraying of liquids may be the following conclusion: if the physical parameters are

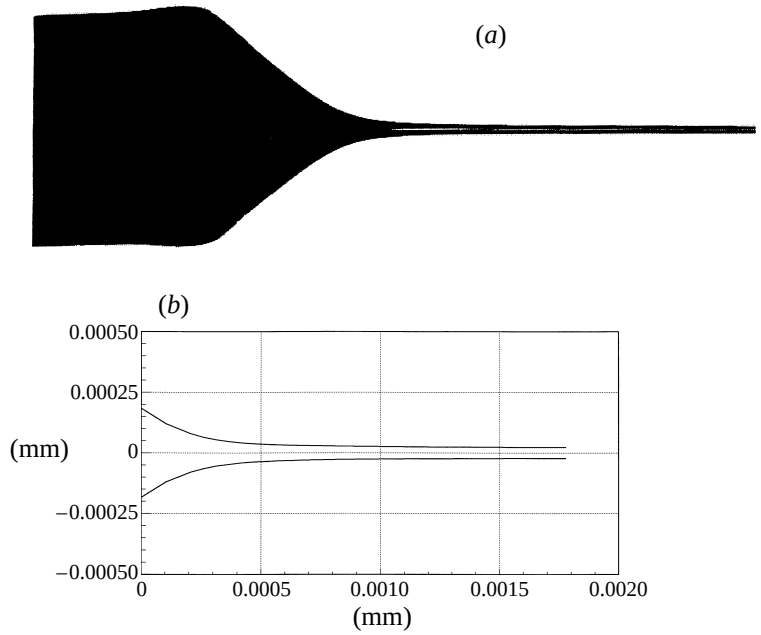

FIGURE 2. (*a*) A photograph of an electrohydrodynamically driven jet issuing from a metallic needle. The experimental conditions are given in §3. (*b*) A plot of the digitized and adjusted shape in the region of interest, using an eighth-order hyperbolic regression.

such that the jet is supercritical from the beginning, it remains supercritical and, therefore, insensitive to downstream (mechanical) boundary conditions.

2.3. *Further extension of the one-dimensional model: jets undergoing self-induction, Taylor's jets*

Here, the difference with the model in §2.2 lies in the outer electric field. When the electrode's radius R_2 becomes comparable to the characteristic jet's length L, the expression for the tangential electric field E_z on the jet's surface is not as simple as that given by (2.11). In this case, most regions of the outer domain of the electric field are now under the direct influence of the whole charge distribution at the axis represented by the jet, whereas only a short region whose axial length is of the order of $R_2 \ll L$ was under the direct influence of a certain point of the jet (see figure 1*a*) in the previous configuration, which precluded the appearance of a self induction effect. In a more general situation, the jet is under the influence of its own electric field, which couples the values of the jet's radius and its charge at each point with those at the other points. The present work is principally aimed at showing why Taylor's jets, genuinely self-inductive and presenting an important surface charge convection, present such remarkable steadiness and stability: it is related to the supercritical nature of the flow almost from the beginning of the jet. Thus, the jet and its electric current are almost insensitive to (i) the breakup perturbations at its end, and (ii) changes in the downstream boundary conditions such as the collocation of the grounded electrode that the jet strikes (or passes through a hole in it) before it breaks up into droplets (see figure 1*b*).

For illustrative purposes, the physical configuration of the jet under study is that given in figure 2. Closing of the system of equations (2.4)–(2.7) requires the self-consistent solution of the external electric field for this geometry. Several authors

have undertaken this problem within certain simplifications (e.g. see Jones & Thong 1971, who neglect the presence of the liquid jet and spray for calculating the needle-to-plate electrostatic field). Much more recently, Pantano, Gañán-Calvo & Barrero (1994) solved numerically for the first time the electrostatic problem of a pointed meniscus attached to a metallic needle in a point-to-plane configuration, also in the limit of a negligible space charge owing to charge emissions (in the form of liquid jet, droplets or ions). In the present work, the presence of the jet invalidates such approximations neglecting the space charge between needle and plate, and the jet problem must be solved together with the needle–plate boundary conditions.

In spite of the intrinsic difficulty of the problem, there are still analytic ways to find, at least formally, closed expressions for the outer electric field in the case of slender quasi-cylindrical geometries.

2.3.1. *Analytical expressions for the outer electric field*

Among the most suitable methods for solving such an involved problem are the spectral ones, owing to the common analytic behaviour of the form $\log(r)$ that the spectral functions present close to the axis of symmetry, either using cylindrical, spherical or any other coordinates having axial symmetry. Furthermore, among the several possible systems of coordinates, experience shows that a suitable choice is the use of spherical coordinates (R, θ) centred either at the tip of the conical shape giving rise to the jet, or at the mouth of the feeding needle if the jet can be considered almost one-dimensional from the beginning (see figure 1*b*).

Without lost of generality, let us assume that the jet extends for $\theta \longrightarrow \pi$ $(R > 0)$, since the position of the origin can be chosen. Therefore, for the steady jet's radius ξ we have

$$\frac{\xi}{R} = \arctan(\pi - \theta_S) \approx (\pi - \theta_S) \tag{2.23}$$

at the points (R, θ_S) defining the jet's shape. In order to keep the quasi-one-dimensionality hypothesis valid in the region of interest, R must be larger than a given $\alpha > 0$ such that ξ/α may still be considered small (of the order of the maximum admissible errors). This point should be taken into account when defining the position of the origin (see figure 1*b*).

The electric potential at the surface can be expressed in the form (Appendix B):

$$\phi_s(R) = B(R) - A(R)\log(\pi - \theta) \approx B(R) - A(R)\log(\xi/R) \tag{2.24}$$

where $B(R)$ and $A(R)$ are not independent functions: they are related through the boundary conditions, as shown by expression (B 5). The dimensional function $A(R)$ is related to the jet's charge per unit length by

$$A(R) = \frac{\sigma_e(R)}{2\pi\varepsilon_o}\left[1 + O(\xi/R) + O(\beta E_n^i/E_n^o)\right] \approx \frac{\sigma_e(R)}{2\pi\varepsilon_o} \tag{2.25}$$

since the normal electric field E_n^o on the surface is

$$E_n^o = -\frac{1}{R}\frac{\partial\phi}{\partial\theta}\bigg|_{\theta_S} \frac{A(R)}{\xi}\left[1 + O(\xi/R)\right] \approx -\frac{1}{R}\frac{\partial\phi}{\partial\theta}\bigg|_{\theta_S} \frac{A(R)}{\xi}. \tag{2.26}$$

The non-singular part $B(R)$ of the outer electric potential contains both the electrostatic solution close to the axis in the total absence of the jet (e.g. the one due to the needle, or the far region of the electrostatic cone in the cone–jet configuration, Cloupeau & Prunet-Foch 1989; Gañán-Calvo *et al.* 1994), and the non-singular part

of the electric potential due to the jet's presence. Thus, let us write $B(R)$ as

$$B(R) = B_o(R) + B_1(R) \tag{2.27}$$

where $B_o(R)$ is such that $\mathrm{d}B_o/\mathrm{d}A \simeq 0$ (being $B_o \neq 0$ in the total absence of the jet). In this work, function $B_o(R)$ is assumed known.

The axial coordinate z can now be identified with R within errors of the order of $(\xi/R)^2 \ll 1$. Thus, the equation for the tangential electric field at the jet's surface can be written in a formal way as

$$E_R = \xi\left[\log\left(\frac{\xi}{R}\right) - \frac{\mathrm{d}B_1}{\mathrm{d}A}\right]\frac{\partial E_n^o}{\partial R} + E_n^o\left[1 + \log\left(\frac{\xi}{R}\right) - \frac{\mathrm{d}B_1}{\mathrm{d}A}\right]\frac{\partial \xi}{\partial R} - \frac{\partial B_o}{\partial R} - \frac{\xi E_n^o}{R} \tag{2.28}$$

for the case that a single term of the power series solution considered in Appendix B, equation (B 5), gives enough accuracy in the region of interest. The self-induction effect, absent in Melcher & Warren's model, is now apparent through the additional term represented in a simplified form as $\mathrm{d}B_1/\mathrm{d}A$, which stands for the dependency of the non–singular part $B_1(R)$ of the outer electric potential (close to the axis) on the charge distribution along the axis (self-induction effect). It does not depend on local conditions only, but on those for whole domain when solving the problem self-consistently. There is also a *sui generis*, new self-induction term, $\xi E_n^o/R$, which represent the coupling between θ and R when using spherical coordinates and eigenfunctions to solve the Laplacian for almost cylindrical geometries, even for $|\tan(\theta)| \ll 1$ (it is part of the projection of E_n^o on the surface using spherical coordinates).

The wave speed of perturbations $a^{\pm}$ has the same expression as (2.15) but now a_{CC} is given by

$$a_{CC} = \frac{\varepsilon_o^2(\beta-1)E_n^o E_z}{2\rho K\xi}\left[2 + \frac{1}{\log(\xi/R_2) - \mathrm{d}B_1/\mathrm{d}A}\right] \tag{2.29}$$

which is affected by the existence of self–induction through the term $\mathrm{d}B_1/\mathrm{d}A$.

The steady forms of the equations for the jet's radius ξ and the outer normal electric field E_n^o are now

$$\frac{\mathrm{d}\xi}{\mathrm{d}R} = \frac{-\varepsilon_o E_n^o\left\{E_R\left[1 + 2\left(\log\left(\frac{\xi}{R}\right) - \frac{\mathrm{d}B_1}{\mathrm{d}A}\right)\right] + \frac{\mathrm{d}B_o}{\mathrm{d}R} + \frac{\xi E_n^o}{R}\right\}}{2\rho\left[\log\left(\frac{\xi}{R}\right) - \frac{\mathrm{d}B_1}{\mathrm{d}A}\right](v + a^+)(v - a^-)}\quad , \tag{2.30}$$

$$\begin{aligned}\frac{\mathrm{d}E_n^o}{\mathrm{d}R} = &-\frac{\left[\varepsilon_o(\beta-1)E_R^2 - \rho\left(\frac{Q}{\pi}\right)^2\frac{1}{\xi^4} - \frac{\gamma}{2\xi}\right]\left(E_R + \frac{\mathrm{d}B_o}{\mathrm{d}R} + \frac{\xi E_n^o}{R}\right)}{\rho\xi\left[\log\left(\frac{\xi}{R}\right) - \frac{\mathrm{d}B_1}{\mathrm{d}A}\right](v + a^+)(v - a^-)} \\ &+\frac{\varepsilon_o E_R(E_n^o)^2\left[1 + \left(\log\left(\frac{\xi}{R}\right) - \frac{\mathrm{d}B_1}{\mathrm{d}A}\right)\right]}{\rho\xi\left[\log\left(\frac{\xi}{R}\right) - \frac{\mathrm{d}B_1}{\mathrm{d}A}\right](v + a^+)(v - a^-)}\quad .\end{aligned} \tag{2.31}$$

System (2.30)–(2.31) must be solved subject to the electric boundary conditions at the needle and the jet's end, and to those resulting from the structure of a possible critical point.

2.3.2. *Physical interpretation of the quasi-one-dimensional equations: supercritical region and jet stability*

As pointed out at the beginning of this section, the existence of a supercritical region, where $v > a^-$, is the key for the existence of perfectly steady electrohydrodynamic capillary jets such as the ones that emerge from equilibrium capillary surfaces (Taylor's cones). While the absence of self-induction effects in equation (2.19) prevents the existence of a point where both numerator and denominator in that equation may vanish, the self-induction terms $\xi E_n^o/R$ (strictly positive) and $-\mathrm{d}B_1/\mathrm{d}A$ in equation (2.30), and therefore in equation (2.31), present in Taylor's jets, now allow the existence of such a point. From the critical point downstream, the supercritical region of the jet actually supplies an impenetrable shield for the fragile conical capillary equilibrium meniscus anchored at the needle's mouth protecting it from the violent perturbations caused by the jet breakup occurring where it ends. The electric current may be locally perturbed by a surface deformation, and the local total free energy increment due to the perturbation is propagated with a wave speed a^- or a^+ in the upstream or downstream direction respectively, in an analogous way as an acoustic perturbation in a nozzle that provokes a local isentropic perturbation of the gas density. If the perturbation cannot proceed upstream, the jet's shape cannot be influenced by changes in the flow occurring downstream of the critical point. Therefore, since the surface electric convection soon becomes dominant over the bulk conduction current (as will be seen in §3), and the surface current is given by the jet's shape, the total electric current remains almost insensitive to downstream boundary conditions. For this reason, analogously to the nozzle theory, the electric current may be interpreted as being 'choked' at the critical point. This feature may explain the conspicuous invariance of the electric current reported by Fernández de la Mora & Loscertales (1994, figure 1) when the cone–jet approaches the grounded electrode.

The propagation speed of the jet's surface perturbations is therefore similar to the propagation speed of a local density perturbation in a nozzle, except for the difference (small in many cases) in the upstream and downstream wave speed. However, the surface can propagate the perturbation only if it is locally *stable*, i.e. when a^- is *real*, which is possible only if the electric forces (the electrostatic force $\varepsilon_o(E_n^o)^2/2$ and the polarization force $\varepsilon_o(\beta - 1)E_z^2/2$) overcome the destabilizing effect of the surface tension force γ/ξ (see for example Schneider *et al* 1967; Saville 1970; Melcher & Warren 1971; Huebner & Chu 1971; Mestel 1994; among others). Should a^- become complex (or $a_{MW}^2 - a_{CC}^2 < 0$), the capillary jet becomes convectively unstable and breaks up downstream after several wavelengths, depending on the liquid viscosity. Let us call this the 'point of instability', which defines the limit between the supercritical and the breakup regions. As long as this point is far away (downstream from the critical point) the supercritical region is not only protective, in the sense that it precludes the propagation of disturbances upstream, but convectively stable itself.

When the flow rate decreases, the point of instability moves upstream; there is a certain flow rate for which this point gets so close to the critical point that the supercritical barrier breaks down: it is the *global stability* limit of the steady jet; at this flow rate, the flow bifurcates from a steady liquid emission in the form of a capillary jet to a dripping, unsteady regime. However, this simplified picture of the minimum flow rate is actually more involved owing to the rôle of the liquid viscosity in delaying the appearance of surface instabilities, and the influence of not small breakup disturbances over the supercritical region.

The next objective of the present work is to show the existence of such a supercritical region in a real jet using the quasi-one-dimensional model. In order to gain knowledge about the characteristic values of the different electrohydrodynamical effects in the governing equations and their relevance, let us perform an experimental analysis of a typical Taylor's jet. In this experiment, the supercritical nature of a Taylor's jet is shown, and its specific characteristics discussed.

3. Experimental analysis

This experiment, arbitrarily extracted from experimental work in progress, serves as an illustration for the understanding of the phenomenon and for the general scaling of the problem. Instead of solving the complete problem for given liquid properties and boundary conditions, the jet's shape ξ is taken from an actual jet, avoiding the complicated solution of the outer electric field. Therefore, the remaining unknowns v, E_n^o, p, and E_z can be calculated using the steady form of the conservation equations of mass, momentum and charge, and the capillary condition i.e. by solving the following equations:

$$v = \frac{Q}{\pi\xi^2}, \tag{3.1}$$

$$\frac{\xi}{2\varepsilon_o}\frac{\mathrm{d}}{\mathrm{d}z}\left(p + \tfrac{1}{2}\rho v^2\right) = E_n^o E_z, \tag{3.2}$$

$$I = \frac{2Q\varepsilon_o}{\xi}E_n^o + \pi\xi^2 K E_z \tag{3.3}$$

and

$$\frac{\gamma}{\xi} = p + \frac{\varepsilon_o}{2}\left((E_n^o)^2 + (\beta - 1)E_z^2\right). \tag{3.4}$$

This system of equations can be reduced to a first-order ordinary differential equation in E_n^o or v or p or E_z. In Appendix C, system (3.1)–(3.4) is reduced to a differential equation for E_n^o, and the uniqueness of the obtained solution discussed.

Once the 'basic' variables E_n^o, E_z and p are obtained for a given jet shape $\xi(z)$, any other desired EHD quantity can be calculated. For example, the inner electric field E_n^i is given by equation (2.9), the electrostatic force is $\varepsilon_o(E_n^o)^2/2$, the polarization force is $\varepsilon_o(\beta-1)E_z^2/2$, the kinetic energy of the liquid is given by $\rho Q^2/(\pi\xi^2)^2$, etc. The perturbation wave speed $a^{\pm}$ can be calculated using

$$a^{\pm} \simeq \pm\frac{\varepsilon_o^2(\beta-1)E_n^o E_z}{\rho K\xi} + \left[\frac{\varepsilon_o}{2\rho}(E_n^o)^2 + \frac{\varepsilon_o(\beta-1)}{\rho}E_z^2 - \frac{\gamma}{2\rho\xi} - \left(\frac{\varepsilon_o^2(\beta-1)E_n^o E_z}{\rho K\xi}\right)^2\right]^{1/2} \tag{3.5}$$

valid within errors of $O\left(|\log(\xi/L)|^{-1}\right) \ll 1$ (see expression (2.15)), L being a characteristic axial length of the jet. It should be pointed out that, although those errors are small for most of the supercritical region, they grow and become not small when the jet approaches the cone. Therefore the location of the critical point is only approximate when using expression (3.5). The term $\mathrm{d}B_1/\mathrm{d}A$ requires *a priori* the calculation of the external electric field with boundary conditions. Since *all* variables except the perturbation wave speed can be calculated within errors of $O(\xi/L) \ll O\left(|\log(\xi/L)|^{-1}\right)$, for the purposes of this analysis no more accurate expressions for a than (3.5) will be used here.

Figure 2 shows a jet issuing from a stainless steel needle of outer and inner diameters $d_o = 1.20$ mm and $d_i = 0.70$ mm, respectively. The distance from the needle bottom to the grounded plate is $H = 38.50$ mm. The liquid used is 1–octanol, with density, viscosity, surface tension, electrical conductivity and relative permittivity $\rho = 827$ kg s^{-1}, $\mu = 0.0081$ kg m^{-1} s^{-1}, $\gamma = 0.0235$ N m^{-1}, $K = 8.05 \times 10^{-6}$ S m^{-1}, and $\beta = 10.0$, respectively. Surface tension was measured with a digital tensiometer Krüss model K10T, liquid viscosity with a torque viscometer from Brookfield, electrical conductivity with a Microprocessor Conductivity Meter LF 3000 from WTW, and permittivity was calculated using Lide's tables (Lide 1990). All properties were obtained at a constant room temperature, $T = 23°C$. The liquid flow rate was $Q = 4.45 \times 10^{-9}$ m^3 s^{-1}, and the applied voltage to the needle was $V = 4650$ V. The measured emitted current was $I = 70.8$ nA. It is therefore unnecessary to solve the critical point of the flow since the eigenvalue I of the problem is experimentally measured and the actual solution of the problem specified.

The cone–jet's shape, presented in figure 2(a), was digitized using image processing techniques, and adjusted by an eighth-order hyperbolic regression:

$$\xi = \frac{1}{\sum_{n=0}^{8} a_n z^n} \tag{3.6}$$

in the region of interest, a plot of which is shown in figure 2(b).

In the following results, a 'radiography' of the flow is presented once the jet's shape is known. In order to warrant the one-dimensional assumptions, equations (3.1)–(3.4) are solved from the point where the jet's slope is less than 0.2. Some main results are summarized in figure 3.

Figure 3(a) gives a comparison between the normal (E_n^o) and tangential (E_z) components of the outer electric field, and the inner, normal electric field E_n^i. It is apparent that E_n^o is everywhere large compared to E_z (of the order of 100 times smaller in this case). In addition, and which is essential with regard to the most important EHD hypothesis made in this work (the neglect of the charge relaxation effects), the quantity βE_n^i is shown to be 100 to 1000 times smaller than E_n^o. This confirms that charge relaxation effects in the liquid are unimportant in this case. However, it should be pointed out that E_n^i can be of the order of 10–20% of E_n^o for this liquid in limit situations, close to the minimum flow rate for which a steady regime can be achieved.

Figure 3(b) shows v, a^- and a^+. The existence of a point where $v = a^-$ may be observed, at $z_c = 0.675$ mm. In addition, when the jet's shape is analysed in the vicinity of the breakup region, there is a point not shown in the plot where $a^- = 0$ (at $z_a \simeq 3.1$ mm). Downstream of this point, the jet becomes convectively unstable, by means of the capillary Rayleigh's instability. Note the small difference (equal to $2a_{CC}$) between a^- and a^+ in this case ($\beta = 10$).

The electric bulk conduction current is compared with the surface charge advection current in figure 3(c). The bulk conduction becomes dominant over surface advection in the subcritical region, close to the needle. As the flow approaches and passes the critical point, the surface advection increases and become dominant over the bulk conduction. Eventually, close to the breakup region, the surface advection is almost the only charge transport mechanism of the flow. It is worth noting that bulk conduction approaches well (within the experimental errors) an exponential function $I_B \simeq 70.8 \times 10^{-9} \exp(-2z/L)$A, while the electric surface convection is $I_C \simeq$

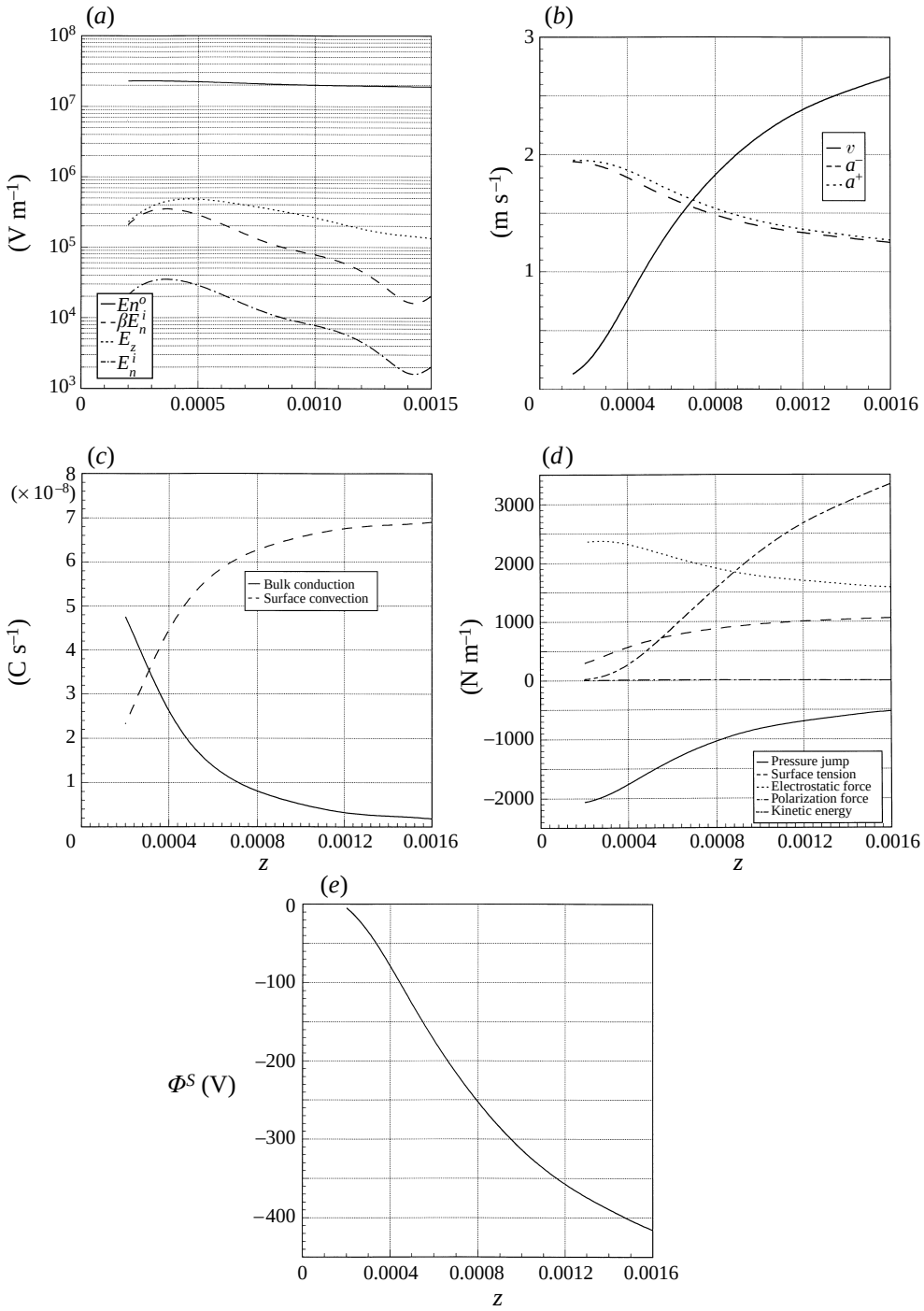

FIGURE 3. (*a*) The normal E_n^o and tangential E_z components of the outer electric field, and the inner, normal electric field E_n^i. (*b*) The square of the liquid velocity v^2 and propagation wave speed of perturbations a^2. (*c*) The surface advection, electric current compared to the Ohmic bulk conduction current. (*d*) Comparison of the kinetic energy of the liquid, pressure jump across the surface, electrostatic forces and the polarization forces in the region of interest. (*e*) Potential decay along the jet in this region, with respect to an arbitrary potential reference.

$70.8 \times 10^{-9}[1 - \exp(-2z/L)]$A, where $L \simeq 0.86$ mm. L can be physically interpreted as an EHD 'global relaxation' length of the problem (not to be confused with bulk electric relaxation), that may be useful for understanding these electrohydrodynamic flows as a transition from a region dominated by, say, 'electrostatics' and bulk electric current, towards another region dominated by 'hydrodynamics' and surface advection current, through a critical point.

A comparison of many important forces of the flow is shown in figure 3(*d*). One of the most apparent features of the subcritical region is the dramatic increase of the kinetic energy of the liquid, at the expense of the electric potential (see figure 3*e*): the tangential electric stress applied on the surface and transmitted to the liquid bulk by viscous stresses experiences a maximum in this region. The pressure jump across the surface, which in the cone seems to be negative owing to electrostatic suction (in this particular case), increases in this region as an indirect consequence of the total amount of momentum being introduced into the liquid by the electric stresses, which is employed in the increase of *both* the liquid inertia and pressure. However, while the liquid inertia is allowed to increase without limit as long as momentum is fed through the liquid surface, the pressure jump is limited by the surface tension force. In fact, the supercritical region is characterized by an increase of the kinetic energy over all other forces represented in figure 3(*d*), while pressure, electrostatic, and surface tension forces balance one each other. Finally, the polarization force $(\beta - 1)E_z^2$ is plotted (almost coinciding with the horizontal axis) just to show how small is it compared to the rest of the forces in this case ($\beta = 10$, moderate or small polarity). Finally, the potential decay along the region here analysed is given in figure 3(*e*).

To guarantee that this experiment is within the limits of the present theory, let us check (1.1) and (1.4) using $L \simeq 0.86$ mm and R_j equal to the jet's diameter at each z point. The maximum value for (1.1) gave

$$\frac{\beta \varepsilon_o Q}{K R_j^2 L} = 0.0098 \ll 1. \tag{3.7}$$

For the viscosity requirements, the limits given by (1.3) are

$$\left(\frac{R_j}{L}\right)^2 \sim 1 \times 10^{-3} \ll \frac{Q}{\nu L} \sim 0.52 \lesssim 1. \tag{3.8}$$

The following conclusions may be drawn from this experimental analysis.

(i) The supercritical nature of an electrohydrodynamically driven jet issuing from a Taylor's cone is, for the first time, experimentally verified. The existence of a critical point almost at the neck joining jet and cone is also shown ($z_c \approx 0.675$ mm in figure 2*b*).

(ii) There is a point where $a^2 = 0$ ($z_a \simeq 3.1$ mm, not shown), from which the small perturbations begin to grow, and they become noticeable at the region close to the breakup point, approximately at $z_b \simeq 3.5$ mm. Therefore, the *supercritical shield* (supercritical and convectively stable flow) extends from $z_c = 0.675$ mm to $z_a = 3.1$ mm.

(iii) The normal component of the outer electric field on the surface is everywhere large compared to the tangential one (almost two orders of magnitude larger, in this experiment).

(iv) The dominant electric current transport is bulk conduction in the subcritical region, when the jet's radius becomes large compared to the critical radius. However,

surface charge advection becomes of the same order as bulk conduction close to the critical point, and eventually, close to the breakup point, the surface charge advection is dominant.

(v) In the supercritical region the pressure jump overcomes the inertia term, and eventually becomes dominant.

(vi) The surface charge layer is actually in quasi–equilibrium conditions: $\beta E_n^i \ll E_n^o$.

(vii) Polarization forces are negligible in this experiment (moderate polarity).

Except for the last one, these conclusions are not specific to this particular experiment. They seem to be rather general for liquids with sufficient conductivity and satisfying the viscous restrictions for the assumption of an almost flat velocity profile (Melcher & Warren 1971, p. 142). Indeed, the author could not find an experimental situation in which one of them failed (except, as mentioned, the last one; a complete experimental analysis, outside the scope of the present work, will be given elsewhere).

4. Conclusions

In this work we have analysed electrohydrodynamically driven jets in the parametrical window corresponding to steady Taylor's jets, namely jets issuing from needles of small diameter, or from equilibrium Taylor's cones (forming the so-called cone–jet mode). A quasi-one-dimensional EHD model retaining the temporal terms, for characteristic times larger than the electrical relaxation times $t_e \sim \varepsilon_o/K$, has been presented. It has been shown that the large axial length-to-diameter ratio of these jets does not allow the convective terms in the charge conservation equation to be neglected. Applying classical techniques, the axial propagation speed of disturbances along the jet's surface has been obtained, showing (i) the supercritical nature of EHD-driven jets issuing from a Taylor's cone, (ii) the existence of a critical point at which the flow changes from a subcritical to a supercritical regime when the electrical self-induction of the jet is not precluded, and (iii) that the upstream wave speed, measured respect to the moving liquid (as usual) is *slower* than the downstream wave speed.

As Melcher & Warren (1971) have already pointed out for their model, EHD-driven jets without self-induction can be either subcritical or supercritical, but they do not have a critical point, and therefore the co-existence of subcritical and supercritical regimes is precluded in these cases: the change from a subcritical regime to a supercritical one takes place as a global bifurcation of the whole flow. However, Taylor's jets are genuinely self-inductive. The conspicuous longevity and stability of these jets is explained in terms of the existence of a *supercritical* and *stable* region of the jet that shields the fragile equilibrium meniscus giving rise to the jet from the strong perturbations produced at the jet's breakup point. This stable region ends at the point at which the upstream wave speed becomes a complex number (point of instability). From this point downstream, the jet is *convectively unstable*, and the small disturbances grow, leading to the eventual jet breakup several wavelengths after that point, depending on the liquid viscosity. Only when the point of instability approaches the critical point (i.e. for small flow rates), does the flow undergo a global bifurcation to a dripping mode.

An experimental study has been also carried out, based on the analysis of a real electrohydrodynamically driven Taylor's jet shape, allowing the quantification of the EHD variables of the problem, the identification of the supercritical region of the jet, and the point of convective instability. The main EHD hypotheses of the present

model are also checked and confirmed in this experiment, within the limits of the one-dimensional assumption.

This work has been supported by the CICYT of Spain (project number PB93-1181) and the Consejería de Educación de la Junta de Andalucía. The author wishes to express his gratitude to Professor A. Barrero for suggesting some penetrating ideas, and for continuous and enriching discussions with him and Dr M. Pérez-Saborid.

Appendix A. Derivation of the perturbation wave speed

The system of first-order partial differential equations (2.4), (2.5), (2.6), (2.18), and either (2.11) or (2.28) can be solved for a perturbation of wavelength λ, such that $R_o \ll \lambda \ll L$, and

$$\frac{\beta Q \varepsilon_o}{K R_o^2 \lambda} \ll 1. \tag{A 1}$$

In this limit, if one writes the dependent variables as

$$\left.\begin{array}{ll} \xi^2 = \xi_o^2 + F_1(z - a^* t), & E_n^o = E_{no}^o + F_2(z - a^* t), \\ E_z = E_{zo} + F_3(z - a^* t), & v = v_o + F_4(z - a^* t), \end{array}\right\} \tag{A 2}$$

where the first term in the right-hand side stands for the stationary value, and $F_i(z - a^* t)$ represent an almost non-dispersive wave (because the characteristic length for the variations of a, of the order of L, is considered large compared to the wavelength λ) with wave speed a^* and wavelength λ, one may write the original system, after some algebra and neglecting terms of order F_i/L compared to the ones of order F_i/λ, as

$$(v_o - a^*)\dot{F}_1 + \xi_o^2 \dot{F}_4 = 0, \tag{A 3}$$

$$(v_o - a^*)\dot{F}_4 - \frac{1}{2\rho}\frac{\gamma}{\xi_o^3}\dot{F}_1 - \frac{\varepsilon_o}{\rho}E_{no}^o \dot{F}_2 - \frac{\varepsilon_o(\beta - 1)}{\rho}E_{zo}\dot{F}_3 = 0, \tag{A 4}$$

$$\xi(v_o - a^*)\dot{F}_2 + \frac{K}{2\varepsilon_o}(\xi_o^2 \dot{F}_3 + E_{zo}\dot{F}_1) = \frac{E_{no}^o}{2\xi_o}(v_o - a^*)\dot{F}_1, \tag{A 5}$$

and, for the extended Melcher & Warren model:

$$\xi_o \log\left(\frac{\xi}{R_2}\right)\dot{F}_2 + \frac{E_{no}^o}{2\xi_o}\left(\log\left(\frac{\xi}{R_2}\right) + 1\right)\dot{F}_1 = 0, \tag{A 6}$$

while for the self-inductive one, under the simplification indicated for equation (2.28), one has

$$\xi_o\left(\log\left(\frac{\xi}{R}\right) - \frac{\mathrm{d}B_1}{\mathrm{d}A}\right)\dot{F}_2 + \frac{E_{no}^o}{2\xi_o}\left(\log\left(\frac{\xi}{R}\right) - \frac{\mathrm{d}B_1}{\mathrm{d}A} + 1\right)\dot{F}_1 = 0 \tag{A 7}$$

where the stationary terms satisfying the stationary equations cancel out in the above expressions. This homogeneous system has two eigenvalues, which can be expressed as $a_1^* = v_o + a^+$ and $a_2^* = v_o - a^-$, $a^\pm$ being equal to the perturbation wave speed given by either (2.15) or (2.29) and representing the propagation speed of disturbances in a Lagrangian frame moving with the surface's velocity. The discussion in Melcher & Warren about this wave speed is applicable here (Melcher & Warren 1971, pp. 133 and 134).

Appendix B. Formal expressions for the outer electric field

The outer electric potential can be formally expressed in terms of discrete series of Legendre and modified Legendre functions $P_v(\theta)$ and $Q_v(\theta)$, respectively, as†

$$\phi(R,\theta) = \sum_v (A_v R^v + A'_v R^{-(v+1)}) \, [Q_v(\theta) + C_v P_v(\theta)] \tag{B 1}$$

where $\{v\}$ is a numerable, infinite set in $\{\mathbb{R}\}$ such that the infinite sequence of powers $\{\mathbb{R}^v\}_{\{v\}}$ ($v < 0$) is complete in the interval $R \in (a, \infty)$, $a > 0$ (i.e. the set $\{v\}$ should verify the hypothesis of Müntz's theorem, Müntz 1914). In this expression, the terms $A'_v R^{-(v+1)}$ can be neglected since (i) for $v \leqslant -1$ they stand for far boundary geometries (such as electrode borders, needle base, etc.) located at distances $L_B \gg L$, and become very small along the jet's domain, when $O(R) \sim O(L)$, and (ii) for $-1 < v < 0$, the number $-(v+1)$ is negative, and therefore is included in the set $\{v\}$, $v < 0$.

Coefficients C_v can be calculated by analysing the possible asymptotic electrostatic solutions which might apply to the jet upstream (i.e. Taylor's conical solution, 1964; this solution is part of the so-called *cone–jet* mode after Cloupeau & Prunet-Foch 1989), or the electrostatic solution owing to the metallic needle. Here, we do not do this analysis (it will be presented elsewhere) and take C_v as given.

Coefficients A_v represent the charge distribution on the axis for $R \in (a, \infty)$ due to the jet, which is the ultimate solution to our problem. It should be solved together with the conservation equations (2.17), (2.18), and the boundary condition

$$E_R|_{\text{surface}} = -\left.\frac{\mathrm{d}\phi}{\mathrm{d}R}\right|_{R_{\text{surface}}} \tag{B 2}$$

The total electric current I is an *eigenvalue* of the problem, analogous to the gas flow rate through a choked convergent–divergent nozzle, which is given by the structure of the critical point and the particular solution passing through it. This solution is not obtained in this work since it is mostly focused on the new physical aspects in the natural extension of Melcher & Warren's model.

The self-induction effect will be formally obtained in an explicit way in the following. For $\theta \longrightarrow \pi$, one has

$$P_v(\theta) \to D_{P1}(v) \log(\pi - \theta) + D_{P2}(v), \tag{B 3}$$

$$Q_v(\theta) \to D_{Q1}(v) \log(\pi - \theta) + D_{Q2}(v), \tag{B 4}$$

where constants $D_{P,Q}(\mathrm{u})$ are known. Invoking (2.23), the electric potential at the jet's surface can be expressed as

$$\phi_s(R) = \sum_{\mathrm{v}} A_v R^{\mathrm{v}} \left[\left(D_{Q1}^{(0,\pi)} + C_{\mathrm{v}} D_{P1}^{(0,\pi)} \right) \log(\xi/R) + \left(D_{Q2}^{(0,\pi)} + C_{\mathrm{v}} D_{P2}^{(0,\pi)} \right) \right]. \tag{B 5}$$

In many cases, this series expression may be reduced to a single term with enough accuracy in a given region of the jet. This is used in the text to derive formal expressions for the tangential electric field at the jet's surface and for the wave speed of perturbations.

† The summation sign can be also understood as an *integral sign*, for which expression (B 1) becomes the Mellin inverse transform of A_v.

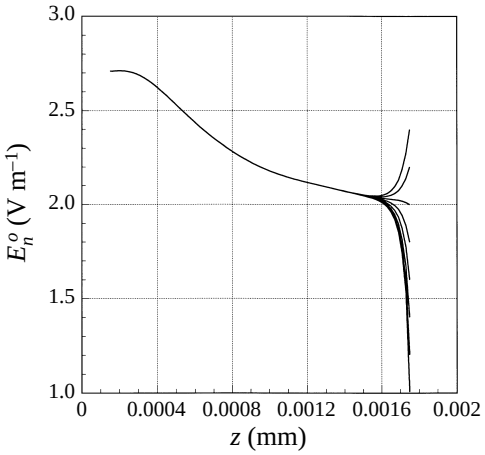

FIGURE 4. Values of the normal electric field on the surface E_n^o as a function of z, for different initial conditions at $z = 1.75$ mm.

Appendix C. Integration of the one-dimensional equations with ξ known

The first step is to identify an appropriate dependent variable to reduce system (3.1)–(3.4) to a single first-order ordinary differential equation. Experience shows that a good choice is to use E_n^o, for which equations (3.1)–(3.4) reduce to

$$\frac{\mathrm{d}E_n^o}{\mathrm{d}z} = \frac{\left[\dfrac{\gamma}{\xi^2} - \dfrac{2(\beta-1)\varepsilon_o I^2}{\pi^2 K^2 \xi^5} - \dfrac{12(\beta-1)Q^2\varepsilon_o^3}{\pi^2 K^2 \xi^7}(E_n^o)^2 + \dfrac{10(\beta-1)Q\varepsilon_o^2 I}{\pi^2 K^2 \xi^6}E_n^o + \dfrac{2\rho Q^2}{\pi^2 \xi^5}\right]}{\dfrac{2Q\varepsilon_o^2 I(\beta-1)}{\pi^2 K^2 \xi^5} - \left[\varepsilon_o + \dfrac{4(\beta-1)Q^2\varepsilon^3}{\pi^2 K^2 \xi^6}\right] E_n^o} \frac{\mathrm{d}\xi}{\mathrm{d}z}$$
$$+ \frac{\dfrac{2\varepsilon_o E_n^o}{\pi \xi^3 K}\left(I - \dfrac{2Q\varepsilon_o}{\xi}E_n^o\right)}{\dfrac{2Q\varepsilon_o^2 I(\beta-1)}{\pi^2 K^2 \xi^5} - \left[\varepsilon_o + \dfrac{4(\beta-1)Q^2\varepsilon^3}{\pi^2 K^2 \xi^6}\right] E_n^o}. \tag{C 1}$$

This equation is integrated from a certain z position (in this case $z = 1.75$ mm) in the upstream direction. Several initial values of the normal electric field are tried, but the actual solution is such a strong attractor for the ODE (integrating in the upstream direction) that it is very soon reached, becoming almost independent of the initial value employed (see figure 4).

REFERENCES

BOGY, D. B. 1981 Steady draw-down of a liquid jet under surface tension and gravity. *J. Fluid Mech.* **105**, 157–176.

CLOUPEAU, M. 1994 Recipes for use of EHD spraying in cone–jet mode and notes on corona discharge effects. *J. Aerosol Sci.* **25**, 1143–1157.

CLOUPEAU, M. & PRUNET-FOCH, B. 1989 Electrostatic spraying of liquids in cone–jet mode. *J. Electrostatics* **22**, 135–159.

CLOUPEAU, M. & PRUNET-FOCH, B. 1990 Electrostatic spraying of liquids: main functioning modes. *J. Electrostatics* **25**, 165–184

DUNN, P. F. & SNARSKI, S. R. 1992 Droplet diameter, flux, and total current measurements in an electrohydrodynamic spray. *J. Appl. Phys.* **71**, 80–84.

Fernández de la Mora, J. & Loscertales, I. G. 1994 The current transmitted by highly conducting Taylor cones. *J. Fluid Mech.* **260**, 155–184.

Gañán–Calvo, A. M., Dávila, J. & Barrero, A. 1997 Current and droplet size in the electrospraying of liquids. Scaling laws. *J. Aerosol Sci.* **28** (in press)

Gañán–Calvo, A. M., Lasheras, J. C., Dávila, J., Barrero, A. 1994 The electrostatic spray emitted from an electrified conical meniscus. *J. Aerosol Sci.* **25**, 1121–1142.

Gomez, A. & Tang, K. 1994 Charge and fission of droplets in electrostatic sprays *Phys. Fluids* **6**, 404–414.

Hayati, I., Bailey, A. & Tadros, Th. F. 1986*a* Investigations into the mechanism of electrohydrodynamic spraying of liquids (I). Effect of electric field and the environment on pendant drops and factors affecting the formation of stable jets and atomization. *J. Colloid Interface Sci.* **117**, 205–221.

Hayati, I., Bailey, A. & Tadros, Th. F. 1986*b* Investigations into the mechanism of electrohydrodynamic spraying of liquids (II). Mechanism of stable jet formation and electrical forces acting on a liquid cone. *J. Colloid Interface Sci.* **117**, 222–230.

Hendricks, C. D. 1962 Charged droplet experiments. *J. Colloid Sci.* **17**, 249–259.

Hendricks, C. D. 1964 An equilibrium value for the charge–to–mass ratio of droplets produced by electrostatic dispersion. *J. Colloid Sci.* **19**, 490–492.

Huebner, A. L. & Chu, H. N. 1971 Instability and break up of charged liquid jets. *J. Fluid Mech.* **49**, 361–372.

Jones, A. R. & Thong, K. C. 1971 The production of charged monodisperse fuel droplets by electrical dispersion. *J. Phys.* D: *Appl. Phys.* **4**, 1159–1166.

Landau, L. D. & Lifshitz, E. M 1960 *Electrodynamics of Continuous Media*. Pergamon.

Lide, D. R. 1990 *CRC Handbook of Chemistry and Physics*, 71st edn. CRC Press.

Melcher, J. R. & Warren, E. P. 1971 Electrohydrodynamics of a current–carrying semi-insulating jet. *J. Fluid Mech.* **47**, 127–143.

Mestel, A. J. 1994 Electrohydrodynamic stability of a slightly viscous jet. *J. Fluid Mech.* **274**, 93–113.

Müntz, H. 1914 *Über den Approximationssatz von Weierstrass, Festschr. H. A. Schwarz*, p. 303. Springer.

Mutoh, M., Kaieda, S. & Kamimura, K. 1979 Convergence and disintegration of liquid jets induced by an electrostatic field *J. Appl. Phys.* **50**, 3174–3179.

Pantano, C., Gañán-Calvo, A. M. & Barrero, A. 1994 Zeroth–order, electrohydrostatic solution for electrospraying in cone–jet mode. *J. Aerosol Sci.* **25**, 1065–1067.

Pfeifer, R. J. & Hendricks, C. D. 1967 Charge-to-mass relationships for electrohydrodynamically sprayed liquid droplets. *Phys. Fluids* **10**, 2149–2155.

Pfeifer, R. J. & Hendricks, C. D. 1968 Parametric studies of electrohydrodynamic spraying. *AIAA J.* **6**, 496–502

Probstein, R. F. 1989 *Physicochemical Hydrodynamics*. Butterworth.

Rayleigh, Lord 1878 On the stability of jets. *Proc. Lond. Math. Soc.* **10**, 4–13.

Saville, D. A. 1970 Electrohydrodynamic stability: Fluid cylinders in longitudinal electric fields. *Phys. Fluids* **13**, 2987–2994.

Schneider, J. M., Lindblad, N. R., Hendricks, C. D. & Crowley, J. M. 1967 Stability of an electrified liquid jet. *J. Appl. Phys.* **38**, 2599.

Shapiro, A. H. 1953 *Compressible Fluid Flow*, vol. I. Ronald Press, NY.

Smith, D. P. H. 1986 The electrohydrodynamic atomization of liquids. *IEEE Trans. Ind. Applics.* **IA-22**, 527–535.

Tang, K. & Gomez, A. 1994 On the structure of an electrostatic spray of monodisperse droplets. *Phys. Fluids* **6**, 2317–2332.

Tang, L. & Kebarle, P. 1991 Effect of the conductivity of the electrosprayed solution on the electrospray current. Factors determining analyte sensitivity in electrospray mass spectrometry. *Anal. Chem.* **63**, 2709–2715

Taylor, G. I. 1964 Disintegration of water drops in an electric field. *Proc. R. Soc. Lond.* A **280**, 383–397

Taylor, G. I. 1969 Electrically driven jets *Proc. R. Soc. Lond.* A **313**, 453–475.

Turnbull, R. J. 1989 Self–acceleration of a charged jet. *IEEE Trans. Ind. Applics.* **25**, 699–704.

VONNEGUT, B. & NEUBAUER, R. L. 1952 Production of monodisperse liquid particles by electrical atomization. *J. Colloid Sci.* **7**, 616–623.

WEBER, V. C. 1931 Zum Zerfall eines Flüssigkeitsstrahles *Z. Angew. Math. Mech.* **11**, 136–154.

ZELENY, J. 1914 The electrical discharge from liquid points, and a hydrostatic method of measuring the electric intensity at their surfaces. *Phys Rev.* **3**, 69–91.

ZELENY, J. 1915 On the conditions of instability of electrified drops, with applications to the electrical discharge from liquid points. *Proc. Camb. Phil. Soc.* **18**, 71–83.

ZELENY, J. 1917 Instability of electrified liquid surfaces. *Phys. Rev.* **10**, 1–6.